Structural Analysis and Normalised Susceptibility Study of Zn Substituted Li-Cu Ferrite

Sujata S. Khot[1,2]*, Neelam S. Shinde[1,2], Nathani Basavaiah[3], Shrikant C. Watawe[4], Milind M. Vaidya[5]

[1]D. B. J. College, Chiplun, India
[2]Smt. Chandibai Himathmal Mansukhani College, Ulhasnagar, India
[3]Indian Institute of Geomagnetism, New Panvel, India
[4]P. D. Karkhanis College, Ambernath (East), India
[5]Vedanta College of Management and Information Technology, Vitthalvadi (West), India
Email: *sujataskhot@rediffmail.com, neelamshinde1976@gmail.com, bas@iigs.iigm.res.in, shrikantwatawe@yahoo.com, milind_chm@yahoo.co.in

Abstract

Lithium ferrites have attracted considerable attention because they have been used as replacements for garnets due to their low cost. A series of polycrystalline ferrite samples with the composition of $Li_xZn_{0.6-2x}Cu_{0.4}Fe_2O_4$ (x = 0.05, 0.1, 0.15, 0.2, 0.25, 0.3) at different chemical reaction temperature (100°C, 125°C and 150°C) were prepared using non-conventional microwave sintering method. The characterization was carried out using X-rays technique. The X-ray analysis confirms the formation of single phase cubic structure. The lattice parameter ranges from 8.3690 Å to 8.4653 Å. The X-ray density shows the variation as a function of temperature of synthesis. The variation of AC susceptibility with temperature shows the existence of single domain structure for $x \geq 0.2$ when the chemical reaction carried at 125°C and 150°C and exhibits super paramagnetic structure for all the composition prepared at 100°C. The samples $x \leq 0.2$ shows multidomain structure for all the samples prepared at 125°C and 150°C. The Curie temperature obtained using the susceptibility data are found to be in the range 350°C to 700°C. An attempt has been made to synthesis the nanoparticles at lower reaction temperature by using non-conventional microwave sintering method.

Keywords

Microwave Sintering, X-Ray Diffraction, Lattice Parameter, AC Susceptibility, Curie Temperature

---

*Corresponding author.

1. Introduction

LiZn and substituted LiZn ferrites have been found to be excellent material in permanent magnets, high density recording media, absorbers and microwave devices due to their low costs, high resistivity and low eddy current loss [1] [2].

In view of the wide ranging applications, mixed lithium zinc ferrites have been chosen for the present study. Substituted lithium ferrites synthesized at lower temperature have advantage of better properties in microwave frequency range [3]. Recently microwave assisted combustion synthesis has emerged as an attractive technique for the production of homogeneous, high purity and crystalline spinel powders. The microwave synthesis is fundamentally different from the conventional synthesis in terms of its heating mechanism. In a microwave oven, heat is generated within the sample volume itself by the interaction of microwaves with the material [4]-[6]. Several studies have been reported on substituted lithium ferrites synthesized using different technique [7]-[9] therefore an attempt has been made in the present communication to report the structural properties of Zn substituted Li-Cu ferrite synthesized using microwave induced combustion synthesis route.

X-ray characterization techniques based on structure and microstructure refinement are usually preferred to determine unit cell dimension, imperfections and the reason for the phase transformations of the synthesized material [10] [11]. The ferromagnetic material shows susceptibility below transformation temperature *i.e.* Curie temperature. The microstructure, grain size play important role in deciding the AC susceptibility. The shape of susceptibility curve has been related by some authors to the domain state of the grains in the sample [12]-[14]. Beside is the thermal variation of AC susceptibility can provide the information about type of anisotropy within the materials and the Curie temperature [15]. In the present work we have investigated the effect of several parameters on the structure of the ferrites and magnetic properties of ferrite. These parameters include the influence of reaction temperature and the effect of microwave treatment.

2. Experimental

Zinc substituted Lithium copper ferrite having general formula of $Li_xZn_{(0.6-2x)}Cu_{0.4}Fe_2O_4$ ($x = 0.05, 0.1, 0.15, 0.2, 0.25, 0.3$) have been prepared at three different chemical reaction temperature using non-conventional microwave sintering method. Ferric Nitrate, Zinc Nitrate, Copper Nitrates, Lithium Nitrate-AR grade were used as the starting material. The stoichiometric proportions of the nitrates were weighed and added in 100 ml of distilled water to produce an aqueous solution. The solution kept in paraffin oil bath at three different chemical reaction temperature 100°C, 125°C and 150°C with constant stirring using the magnetic stirrer for three hours, in which the release of nitrates fumes results into the formation of thick slurry. The slurry was then transformed into the modified microwave oven (Model-GMS 17M07 WHGX). The microwave assisted combustion synthesis involving hydrothermal reactions were carried out in modified domestic microwave oven operating at maximum power output of 700 W. The irradiation was given in the form of pulses for nearly 30 to 32 minutes and the process was stopped when nitrous gases were evaporated completely. Finally the required brown coloured composition is formed. The obtained ferrite powder was then crushed in agate morter.

Formation of ferrite was confirmed by X-ray Diffractometer D 8 Advance (by M/s Bruker AXS), GmbH, Germany, using CuKα ($\lambda = 1.540589$ Å) radiation. Crystal structure was determined from XRD data. AC susceptibility of powdered samples was measured in the temperature range 400°C to 800°C on AGICO KLY-45 set up.

3. Result and Discussion

3.1. X-Ray Diffraction Pattern

Powder X-ray diffractometry of the ferrite samples showing well defined reflections reveal the formation of single phase cubic spinel ferrite. Typical X-ray diffractograms of the compositions are shown in the **Figures 1-3**. It is observed that the positions of the peaks are match with the standard JCPDS [16]-[18] data clearly indicating the single phase formation of the spinel ferrite.

3.2. Lattice Parameter

The lattice parameter of all the samples has been calculated from X-ray data of the [311] diffraction peak. The variation of the lattice parameter with Zn content for all the samples at different reaction temperature is depicted
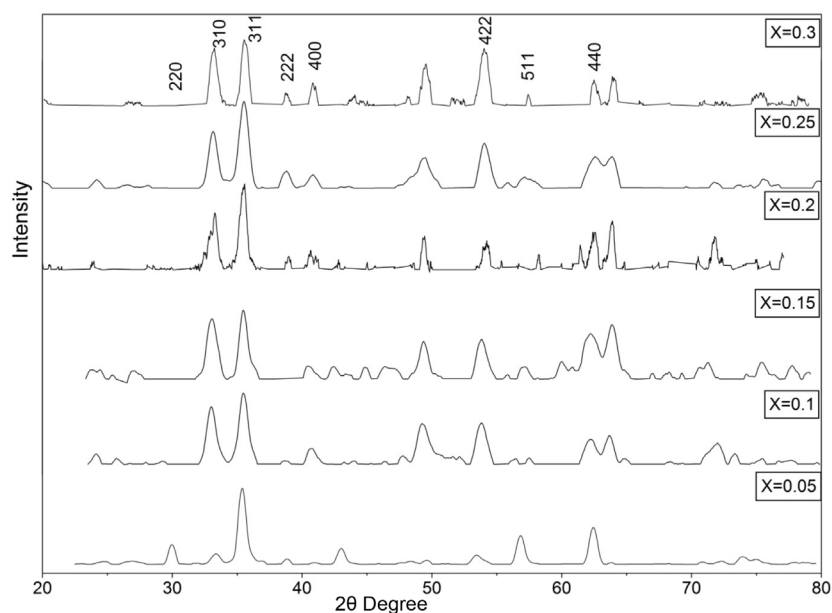
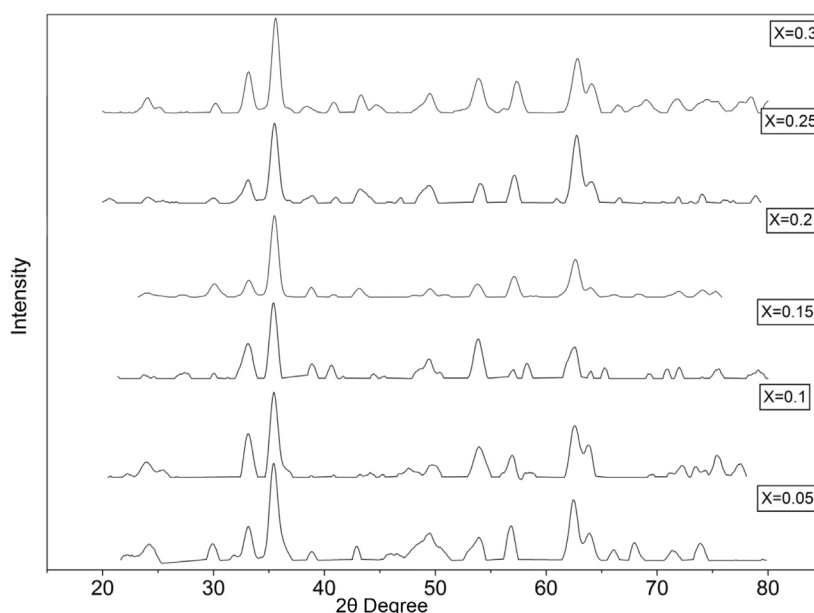**Figure 1.** XRD of the composition—100 Deg.

Figure 2. XRD of the composition—125 Deg.

in **Figure 4**. From figure, it is observed that the value of lattice parameter linearly increase with Zn^{2+} content obeying Vegards law [19]. This may be due to the Zn^{2+} ion having large ionic radius, which when substituted resides on A-site and displaces small Fe^{3+} ion from A-site to the B-site. Similar results for Li-Zn ferrite system have been reported by S. A. Jadhav *et al*. [20]. When ions of larger radii are substituted, this cause a lattice to expand and a linear increase in lattice parameter is therefore expected [21]. This suggests that the occupancy of Zn^{2+} on A site. Similar results are observed in rare earth substituted Li-Zn ferrite system [22].

S. A. Mazen *et al*. [23] have reported the value of lattice parameter in the same range and they have synthesized samples by ceramic method and sintered the samples at 800°C. The results in the present communication are in accordance with the other reported values for Li-Zn composition [20] [22]-[23]. The sample prepared at 100°C shows the greater values of lattice parameter as compared to the samples prepared at 125°C and 150°C.
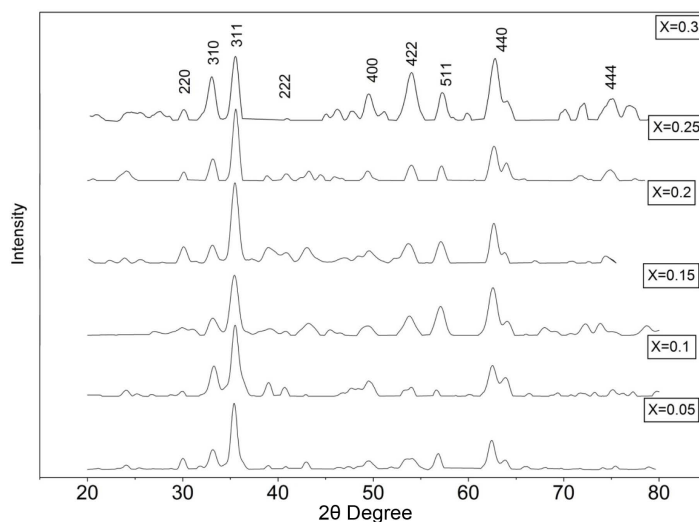
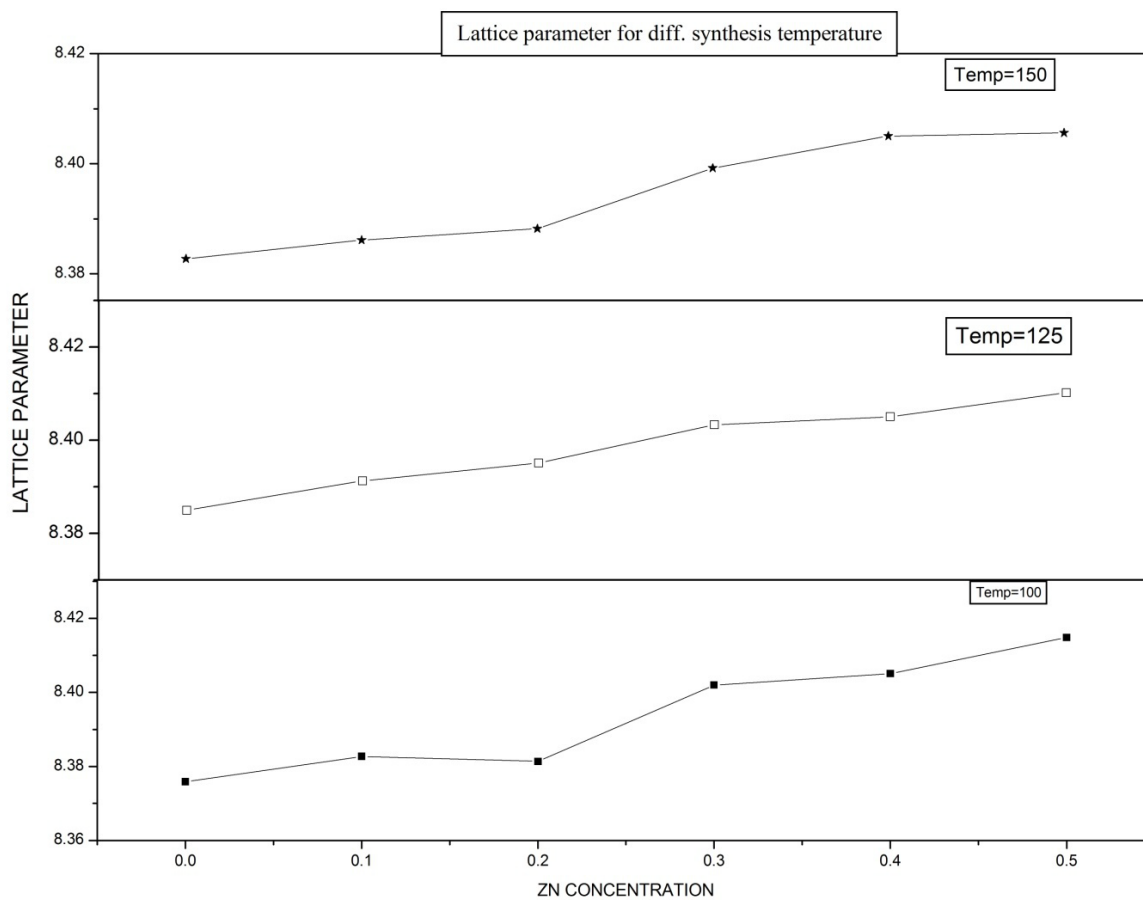**Figure 3.** XRD of the composition—150 Deg.

Figure 4. Lattice parameter with composition.

The value of lattice parameter increases with increase in reaction temperature. This can be attributed to the chemical kinematics [24]. It was found that the rates of most of the chemical reaction increase with temperature therefore it has been found that the temperature at 125˚C and 150˚C have effect on the phase structure, crystal size and lattice constant.

3.3. X-Ray Density

The calculated values of X-ray density are listed in **Table 1**. X-ray density shows the variation as a function of temperature of chemical reaction and with respect to the Zn content. From these values, it is observed that the X-ray density shows increasing trend with increase in Zn concentration. The increase in densities can be ascribed to the atomic weight and density of Zn^{2+} (65.38 and 7.14 gm/cm^3) which are higher than the Li^{2+} (6.939 and 8.96 gm/cm^3), Cu^{2+} (63.564 and 8.96 gm/cm^3) and Fe^{3+} (55.847 and 7.86 gm/cm^3) [25]. The replacement of Fe^3 by larger Zn ion and the molecular wt. has more increment when compared to the volume of the unit cell [25], therefore the X-ray density increases with increase in Zn concentration.

The sample prepared at 100˚C having X-ray density in the range 5.291 gm/cm^3 to 4.999 gm/cm^3 while for samples whose chemical reaction carried out at 125˚C and 150˚C, the X-ray density lies in the range 5.267 gm/cm^3 to 4.987 gm/cm^3 and 5.191 gm/cm^3 to 4.987 gm/cm^3 respectively. As temperature of chemical reaction increases from 100˚C to 125˚C, the X-ray density decrease and again it increase for the temperature 150˚C. The change in X-ray density could be attributed to the temperature dependent activation energy for the reaction *i.e.* reaction kinematics, atomic weight and radii of constituent ions [26]. Similar results are reported by S. A. Mazen *et al.* [23] and Muthafar F. Al-Hilli [27]. S. Manjura *et al.* [25] have reported the value of Dx in the range 4.6 gm/cc to 5.2 gm/cc for Li-Cu mixed ferrite and they synthesized the samples by the solid state reaction method and sintered at 1000˚C.

Particle size for all the compositions shown in **Table 1** was estimated by Scherer's formula [20] given by,

$$t = \frac{0.9\lambda}{B\cos\theta}.$$ (1)

where *t* is the diameter of the crystal particle, λ is the wavelength of the target used (here CuK_α = 1.5418 Å), *B* is the full width at half maximum of diffracted line in radian.

The particle size for all the compositions was observed to vary in the range 18.49 - 41.93 nm, which confirmed that the synthesized powder has nanocrystalline nature. This proved that microwave assisted combustion method results in nanocrystals.

3.4. AC Susceptibility

Polycrystalline magnetic material consists of three types of domain states viz single domain, multi domain and super-paramagnetic [28] For SD samples, χ_{AC} increases and shows maxima at blocking temperature drops sharply to zero at Curie temperature. For MD samples, χ_{AC} remains independent upto a certain temperature and drops sharply at Curie temperature. For SP samples, χ_{AC} decreases with increases in temperature [28].

Based on this inspection, the results of the samples prepared at different reaction temperature are discussed. **Figures 5-7** show the variation of normalized susceptibility against temperature.

1) The sample synthesized at 100˚C: From **Figure 5**, it is observed that the normalized susceptibility decreases with increase in temperature and it falls close to the Curie temperature in the range 400˚C to 660˚C. The composition shows the characteristic of Halfkinson curve [22]. Based on this, it suggests that the composition can be attributed to the existence of SP nature. The explanation of experimentally observed Hopkinson peak

Table 1. Variation of X-ray density and crystalline size with composition and temperature of synthesis.

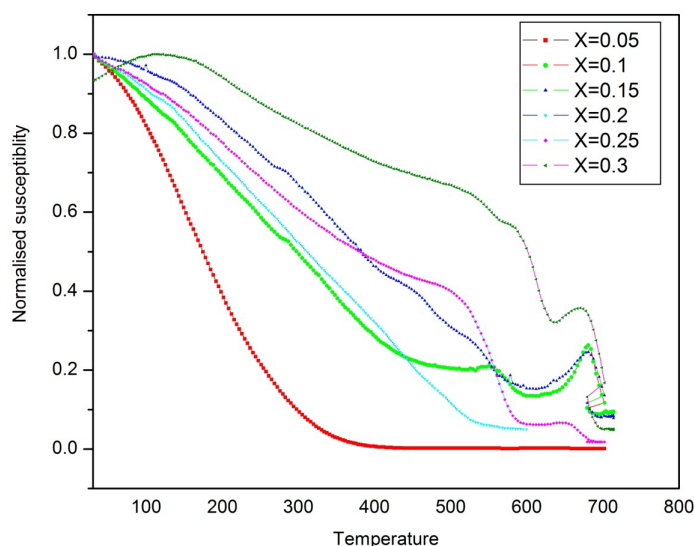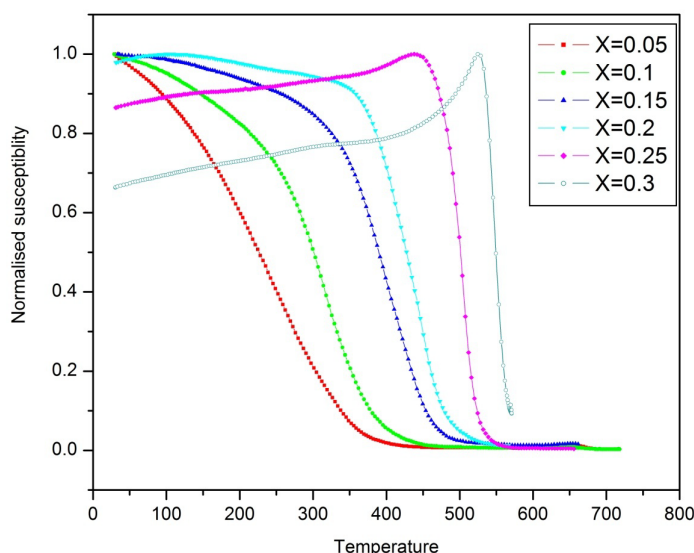| Composition	X-ray density (gm/cm^3)			Crystal size (nm)		
	100˚C	125˚C	150˚C	100˚C	125˚C	150˚C
0.05	5.291	5.263	5.191	34.57	40.90	41.00
0.1	5.282	5.247	5.213	30.13	24.90	30.44
0.15	5.154	5.141	5.167	31.64	37.00	31.54
0.2	5.128	5.103	5.078	30.90	28.19	34.52
0.25	5.027	5.014	5.051	36.01	37.01	33.23
0.3	4.999	4.987	4.987	20.39	18.58	26.22

Figure 5. Normalised susceptiblity 100 Deg.

Figure 6. Normalised susceptiblity 125 Deg.

based on superparamagnetic state at a blocking temperature just below *Tc* is proposed. This peak turns out to be associated with the transition from the region of stable magnetization to super-magnetic state with connection of drastic fall of magnetic anisotropy [29].

2) The sample synthesized at 125˚C: The temperature dependence of the normalized susceptibility for the sample carried the reaction at 125˚C is shown in **Figure 6**. A change in domain structure was observed. The composition $x = 0.05, 0.1$ exhibits SP nature. For the composition $x = 0.1, 0.15$, AC susceptibility has been found independent of temperature and drops off at Curie temperature, which suggests the existence of Multido-main structure [30]. The composition $x = 0.2, 0.25, 0.3$, χ_{AC} increases slowly and shows a peak at blocking tem-perature and drops at Curie point, which suggests the existence of single domain structure [31]. Thus the sample synthesized at 125˚C shows change in structure from SP to MD and then to SD. The composition shows the Cu-rie temperature in the range from 415˚C to 580˚C.

3) The sample synthesized at 150˚C: **Figure 7** shows the variation of AC susceptibility with temperature. It is observed that, the composition $x = 0.05$ exhibits SP nature while $x = 0.1, 0.15, 0.2$ shows MD structure and $x = 0.25, 0.3$ shows SD structure. The Curie temperature lies in the range 400˚C to 600˚C.
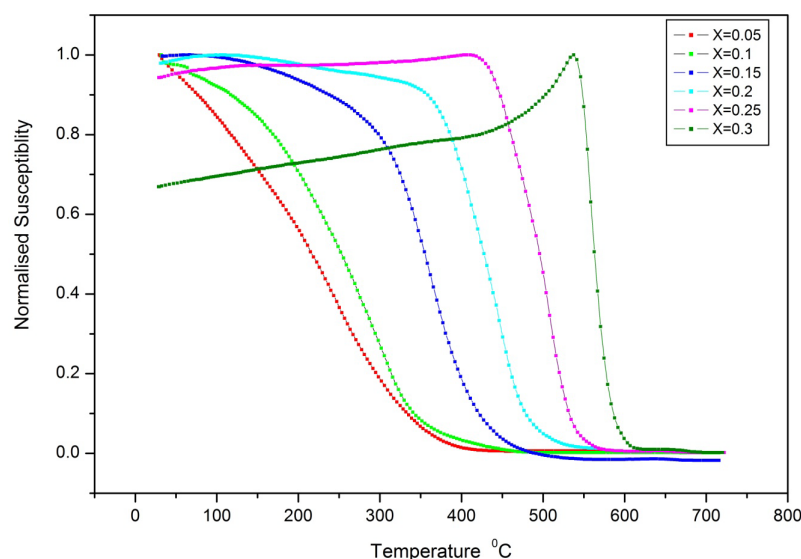
Figure 7. Normalised susceptiblity 150 Deg.

From above discussion, it is observed that the change in domain structure depends on the temperature of chemical reaction and substituted Zn concentration. For lower concentration of Zn, sample x = 0.2, 0.25, 0.3 shows single domain, and x = 0.15, 0.1 exhibits multidomain structure. The high concentrated Zn samples, x = 0.05, 0.1 shows SP nature.

Sample prepared at 100°C exhibits SP nature. As temperature of reaction increases to 125°C and 150°C, sample exhibits single domain and multidomain structure. This can be attributed to chemical kinematics. Increasing chemical reaction temperature, increases reaction rates because of the disproportionately large increase in the number of high energy collisions. Collisions only result in a reaction if the particles collide with enough energy to get the reaction started. This minimum energy required is called the activation energy for the reaction [25].

4. Conclusion

Single spinel phases of Zn-substituted Li-Cu ferrite are studied. Li-Zn-Cu ferrite samples with different composition have been prepared using low temperature microwave assisted combustion method. The effects of synthesis temperature on the structure were investigated. The X-ray diffraction patterns of all the samples have confirmed the formation of single phase spinel cubic structure. The substitution of Zn in host lattice alters the domain structure SD to SP. The samples synthesized at 150°C showing better results as compared to other results. This method avoids using traditional high temperature synthesis and high temperature sintering and therefore could be easily extended to other system.

Acknowledgements

References

[1]   Pardavi-Horvath, M. (2000) Microwave Applications of Soft Ferrites. *Journal of Magnetism and Magnetic Material*, **215**, 171-183. http://dx.doi.org/10.1016/S0304-8853(00)00106-2

[2]   Yusoff, A.N. and Abdullah, M.H. (2004) Microwave Electromagnetic and Absorption Properties of Some LiZn Ferrites. *Journal of Magnetism and Magnetic Material*, **269**, 271-280. http://dx.doi.org/10.1016/S0304-8853(03)00617-6

[3]   Watawe, S.C., Keluskar, S., Gonbare and Tangasali, R. (2006) Preparation and Magnetic Properties of Cadmium Substituted Lithium Ferrite Using Microwave-Induced Combustion. *Thin Solid Films*, **505**, 168-172. http://dx.doi.org/10.1016/j.tsf.2005.10.032

[4] Verma, S., Joy, P.A., Khollam, Y.M., Potdar, H.S. and Deshpande, S.B. (2004) Synthesis of Nanosized MgFe$_2$O$_4$ Powders by Microwave Hydrothermal Method. *Materials Letters*, **58**, 1092-1095. http://dx.doi.org/10.1016/j.matlet.2003.08.025

[5] Komarneni, S., Roy, R. and Li, Q.H. (1992) Microwave-Hydrothermal Synthesis of Ceramic Powders. *Materials Research Bulletin*, **27**, 1397. http://dx.doi.org/10.1016/0025-5408(92)90004-J

[6] Komarneni, S., Roy, R., Li, Q.H., Stefanson, K.M. and Roy, R. (1993) Hydrothermal Processing of Synthesis of Electroceramics Powder. *Journal of Materials Research*, **8**, 3176. http://dx.doi.org/10.1557/JMR.1993.3176

[7] Bellad, S.S., Pujar, R.B. and Chougule, B.K. (1998) Structural and Magnetic-Properties of Some Mixed Li-Cd Ferrites. *Material Chemistry and Physics*, **52**, 166-169. http://dx.doi.org/10.1016/S0254-0584(98)80019-9

[8] Ravinder, D. (1992) Dielectric Behaviour of Mixed Lithium-Zinc Ferrites. *Journal of Materials Science Letters*, **11**, 1498-1500. http://dx.doi.org/10.1007/BF00729271

[9] Akhatar, S. and Hakim, M.A. (2010) Magnetic Properties of Cadmium Substituted Lithium Ferrite. *Material Chemistry and Physics*, **120**, 399-403. http://dx.doi.org/10.1016/j.matchemphys.2009.11.023

[10] Patange, S.M., Shirsath, S.E., Jangam, G.S., Lohar, K.S., Jadhav, S.S. and Jadhav, K.M. (2011) Rietveld Structure Refinement, Cation Distribution and Magnetic Properties of Al^{3+} Substituted NiFe$_2$O$_4$ Nanoparticles. *Journal of Applied Physics*, **109**, Article ID: 053909. http://dx.doi.org/10.1063/1.3559266

[11] Pradhan, S.K., Bid, S., Gateshki, M. and Petkov, V. (2005) Microstructure Characterization and Cation Distribution of Nanocrystalline Magnesium Ferrite Prepared by Ball Milling. *Materials Chemistry and Physics*, **93**, 224-230. http://dx.doi.org/10.1016/j.matchemphys.2005.03.017

[12] Radhakrishnamurthy, C. and Nandikar, N.G. (1979) Inhibition of Domain Wall Formation and Its Effects on the Bulk Magnetic Properties of Certain Spinels. *Pramana*, **13**, 413-422. http://dx.doi.org/10.1007/BF02846138

[13] Chougule, R.S., Radhakrishnamurthy, C., Sampathkumaran, E.V.S., Malik, S.K. and Vijayaraghvan, R. (1983) AC Magnetic Susceptibility and Hysteresis Studies on La$_{1-x}$Y$_x$Mn$_2$Si$_2$ Intermetallic Compounds. *Materials Research Bulletin*, **18**, 817-821.

[14] Jadhav, S.R., Sawant, S.R., Suryawanshi, S.S., Patil, S.A. and Patil, R.N. (1989) *Proceedings of* 5*th International Conference on Ferrites*, **1**, 453.

[15] Bhosale, D.N., Verenkar, V.M.S., Rane, K.S., Bakare, P.P. and Sawant, S.R. (1999) Initial Susceptibility Studies on Cu-Mg-Zn Ferrites. *Materials Chemistry and Physics*, **59**, 57-62. http://dx.doi.org/10.1016/S0254-0584(99)00028-0

[16] Bastin, *et al.* (1974) *Zeitschrift für Metallkunde*, **65**, 656.

[17] Hanawalt, J.D., Rinn, H.W. and Frevel, L.K. (1938) Chemical Analysis by X-Ray Diffraction. *Analytical Chemistry*, **10**, 475-512.

[18] Waldo, G. (1935) *American Mineralogist*, **20**, 590.

[19] Cullity, B.D. (1978) Elements of X-Ray Diffraction. Addison-Wesley, Reading.

[20] Jadhav, S.A. (2000) Structural and Magnetic Properties of Zn Substituted Li-Cu Ferrites. *Materials Chemistry and Physics*, **65**, 120-123. http://dx.doi.org/10.1016/S0254-0584(00)00221-2

[21] Soibam, I., Phanjoubam, S., Sharma, H.B. and Sarma, H.N.K. (2008) Effects of Cobalt Substitution on the Dielectric Properties of Li-Zn Ferrite. *Solid State Communications*, **148**, 399-402.

[22] Reddy, P.V.B., Reddy, V.R., Gupta, A., Gopalan, R. and Reddy, C.G. (2008) Mössbauer Study of Nano-Crystalline Li-Ni Ferrite. *Hyperfine Interactions*, **183**, 81-86. http://dx.doi.org/10.1007/s10751-008-9733-6

[23] Mazen, S.A. and Elmosalami, T.A. (2011) Structural and Elastic Properties of Li-Ni Ferrite. *ISRN Condensed Matter Physics*, **2011**, Article ID: 820726.

[24] Bhatt, S.M., Deogadkar, B.B., Jadhav, H.V., Patil, L.S. and Joshi, K.M. (2012) Chemistry Part-I, XII, Maharashtra State Board of Secondary & Higher Secondary Education.

[25] Hoque, S.M., Ullah, M.S., Khan, F.A., Hakim, M.A. and Saha, D.K. (2011) Structural and Magnetic Properties of Li-Cu Mixed Spinel Ferrites. *Physica B*: *Physics of Condensed Matter*, **406**, 1799-1804.

[26] Jing, J., Li, L. and Xu, F. (2007) Structural Analysis and Magnetic Properties of Gd-Doped Li-Ni Ferrites Prepared Using Rheological Phase Reaction Method. *Journal of Rare Earths*, **25**, 79-83.

[27] Al-Hilli, M.F., Li, S. and Kassim, K.S. (2009) Microstructure, Electrical Properties and Hall Coefficient of Europium-Doped Li-Ni Ferrite. *Material Science and Engineering*, **158**, 1-6. http://dx.doi.org/10.1016/j.mseb.2008.12.022

[28] Ladgaonkar, B.P., Vasambekar, P.N. and Vaingankar, A.S. (2000) Effect of Zn^{2+} and Nd^{3+} Substitution on Magnetization and AC Susceptibility of Mg Ferrite. *Journal of Magnetism and Magnetic Materials*, **210**, 289-294. http://dx.doi.org/10.1016/S0304-8853(99)00468-0

[29] Sláma, J., Šoka, M., Grusková, A., Gonzalez, A. and Jančárik, V. (2011) Hopkinson Effect Study in Spinel and Hex-

agonal Ferrites. *Journal of Electrical Engineering*, **62**, 239-243.

[30] Lipare, A.Y., Vasambekar, P.N. and Vaingankar, A.S. (2003) A.C. Susceptibility Study of CaCl$_2$ Doped Copper-Zinc Ferrite System. *Bulletin of Materials Science*, **26**, 493-497. http://dx.doi.org/10.1007/BF02707346

[31] Vasambekar, P.N., Kolekar, C.B. and Vaingankar, A.S. (1998) Cation Distribution and Susceptibility Study of Cd-Co and Cr^{3+} Substituted Cd-Co Ferrites. *Journal of Magnetism and Magnetic Materials*, **186**, 333-341. http://dx.doi.org/10.1016/S0304-8853(98)00099-7